VIA MEDICA

Nuclear Medicine Review 2023, 26, 123–129
DOI: 10.5603/nmr.93300
Copyright © 2023 Via Medica
ISSN 1506–9680, e-ISSN 1644–4345

Original

Analysis of the utility of 2-[^{18}F]FDG PET/CT in the diagnosis of vascular graft infection

Jakub Mitura[1, 2], Beata E. Chrapko[1], Marek Chrapko[3]

[1]Department of Nuclear Medicine, Medical University of Lublin, Lublin, Poland
[2]National Information Processing Institute, Warsaw, Poland
[3]Department of Vascular Surgery, Stefan Kardynał Wyszyński Province Specialist Hospital, Poland

[Received 3 I 2023; Accepted 17 VIII 2023]

Abstract

Background: As a result of constantly improving surgical methods, an increasing number of patients have medical devices implanted in the cardiovascular system (including vascular grafts and endografts). Such patients are characterised by their high risk of infectious complications due to the possibility of biofilm formation on implanted material. This work aims to analyse the utility of 2-[^{18}F]FDG PET/CT in diagnosing vascular graft and endograft infections.

Material and methods: The study was undertaken on a group of 58 patients, of whom 34 were in the study group, and 24 were in the control group. The 2-[^{18}F]FDG PET/CT study was conducted in the Nuclear Medicine Department at the University Hospital of Lublin. The inclusion criteria for the study group were the presence of a vascular graft or endograft that encompasses the aorta, and strong clinical suspicion of its infection. The inclusion criteria for the control group were the presence of a vascular graft or endograft in the large arteries and the absence of signs of its infection on 2-[^{18}F]FDG PET/CT, as well as the absence of clinically apparent signs and symptoms during six months of observation after 2-[^{18}F]FDG PET/CT. All patients found in the database that met the criteria were included.

Results: Vascular endografts were more common in the control group than in the study group. However, in the case of infection of the vascular endograft, signs of infection in 2-[^{18}F]FDG PET/CT were more severe. Images in the study group were divided into three groups that represent image patterns based on CT and PET characteristics. The first pattern (P1) was recognised in six patients. The second (P2) and third (P3) were visible in 11 and 17 patients, respectively.

Conclusions: Comparative analysis of the study and control groups demonstrates the utility of 2-[^{18}F]FDG PET/CT in the diagnosis of vascular graft/endograft infection.

KEY words: blood vessel prostheses; positron emission tomography/computed tomography; infections

Nucl Med Rev 2023; 26, 123–129

Introduction

As a result of pathologies in the cardiovascular system, some patients must undergo the procedure of implantation of vascular graft (VG) or vascular endograft (VE), jointly referred to later as VGE or vascular prostheses. Such devices can be implanted both through intravascular methods and during open surgery. Both types of procedures require different types of VGE, and, in the case of endovascular aneurysm repair (EVAR), VE must be used. Every kind of VGE has a different set of advantages and disadvantages.

The most common causes of implantation of VGE are aneurysms and constriction/closing of the arteries, usually caused by atherosclerosis.

Correspondence to: Jakub Mitura, Department of Nuclear Medicine, Medical University of Lublin, Jaczewskiego 8C, 20–090 Lublin, Poland; phone: +48 81724 4339; e-mail: jakub.mitura14@gmail.com

Although the prevalence of vascular graft infection is low (0.5–5%) [1], it is associated with a high risk of death (20–75%) and limb amputation [1]. Depending on the type of VGE, its infection can be divided into vascular graft infection (VGI) and vascular endograft infection (VEI) jointly referred to later as VGEI.

Diagnosis of VGEI is usually complex and requires a multidisciplinary team. Typically, the physical examination, laboratory data, and patient history are insufficient to confirm or rule out infection diagnosis. For this reason, the role of diagnostic imaging is crucial. Nevertheless, the most commonly performed classical radiological studies are not devoid of shortcomings. The main one is that they can only assess the changes in the anatomy and not the character and intensity of pathophysiological processes present. This is particularly important in the early stages of infection (as metabolic changes generally precede anatomical ones) and in low-intensity chronic conditions. Nuclear medicine studies that can assess the metabolic state of tissue are emerging as crucial in early diagnosis.

This article is available in open access under Creative Common Attribution-Non-Commercial-No Derivatives 4.0 International (CC BY-NC-ND 4.0) license, allowing to download articles and share them with others as long as they credit the authors and the publisher, but without permission to change them in any way or use them commercially.

One of the most commonly used techniques in infection and inflammation imaging is the 2-[^{18}F]fluoro-2-deoxy-D-glucose positron emission tomography/computed tomography (2-[^{18}F]FDG PET/CT) study. This technique enables high-resolution and hybrid imaging, which combines molecular and anatomical imaging into a single study and leads to diagnostic performance gains more significant than the sum of two separate studies. Visual inspection of 2-[^{18}F]FDG PET/CT is based on searching for glucose uptake abnormalities that concern the anatomical structure discerned by a computed tomography (CT) scan.

Aim

This work expands upon a previous article published in 2020 by the same team [2] (briefly mentioned in the discussion). The study group is now significantly larger (34 *vs.* 24) and incorporates a control group (24 patients). Due to increased data size and quality, new statistical and qualitative analysis types could be performed. This work's primary goal is to analyse the utility of 2-[^{18}F]FDG PET/CT in diagnosing VGEIs.

Material and methods

Patients and design

The study was undertaken on 58 patients, of whom 34 were in the study group, and 24 were in the control group. All patients underwent a 2-[^{18}F]FDG PET/CT study in the Nuclear Medicine Department of the University Hospital of Lublin.

The study group comprised 4 females and 30 males with a median age of 65 (IQR 11.25). The longest duration between the vascular procedure and the 2-[^{18}F]FDG PET/CT study was 61.1 months, and the shortest was 0.6 months. The inclusion criteria for the study group were the presence of a VGE that encompasses the aorta and strong clinical suspicion of VGEI. The most common cause of vascular procedure was aortic aneurysm (N = 26); patients (in other cases N = 5) had undergone vascular procedure due to atherosclerosis, including Leriche syndrome (N = 3), or infection of a previously implanted VGE. In 26 cases, implantation had been performed in the abdominal aorta and in eight cases in the ascending aorta (all the cases of the vascular graft in the ascending aorta were implanted using the Bentall procedure). EVAR using VE implantation was performed on 14 patients, while open surgery was performed on 20 patients.

Patients for the control group were collected retrospectively by analysis of the digital base of the nuclear medicine department. The inclusion criteria were the presence of a VGE in the large arteries and the absence of signs of infection around the VGE like focally increased activity of 2-[^{18}F]FDG in PET/CT study, as well as the absence of clinically apparent signs and symptoms of infection within six months of observation after 2-[^{18}F]FDG PET/CT. All patients found in the database that met the criteria were included. Patient data was acquired based on medical documentation, or contact with either the patient or the leading physician. Most control group patients were referred to the nuclear medicine department for routine oncological reasons.

In 16 cases, implantation was performed in the abdominal aorta, three in the ascending aorta and three in the iliac arteries, one bypass graft between the femoral arteries, and one in the femoral artery. Endovascular procedures were performed on 19 patients; in five cases, VG was implanted via open surgery. Data on the study and control groups are summarised in Table 1.

Table 1. Characteristics of patients in the study and control groups

	Study group (n)	Control group (n)
Number of patients, n [%]	34 (100)	24 (100)
Females, n [%]	4 (12)	3 (13)
Males, n [%]	30 (88)	21 (88)
Median age	61	72
Abdominal aorta loc.*, n [%]	26 (76)	16 (67)
Thoracic aorta loc.*,n [%]	8 (24)	3 (13)
Other loc.*, n [%]	0 (0)	5 (21)
VE, n [%]	14 (41)	19 (79)
VG, n [%]	20 (59)	5 (21)

*location of VGE; VE — vascular endograft, VG — vascular graft

Patient preparation

The patients were advised to limit their carbohydrate intake for 24 hours before the study and to fast for at least six hours before the examination, as well as avoid strenuous exercise, alcohol consumption, and cigarette smoking for 24 hours before. They were also asked to attend the study in warm and comfortable clothing. Glucose levels were measured before the administration of a radiotracer. Its median value in the study group was 103.5 (IQR 24.0) mg%; in the control group, the median was 89.5 (IQR 29.75) mg%. In the case of diabetic patients, at least a four-hour interval between the administration of insulin and the beginning of the study was ensured.

2-[^{18}F]FDG PET/CT

The 2-[^{18}F]FDG PET/CT study was performed 60 minutes after the intravenous injection of 2-[^{18}F]FDG (3.5 MBq per kilogram of body weight), mean activity 241.5 MBq, range 198–334 MBq, in the supine position, with upper limbs placed above the head. The study's field of view ranged from the top of the head to the mid-thigh, except for that of patients with VGE placed in the lower limbs; in such cases, the field of view was suitably extended. All studies were performed using a PET/CT Biograph mCT S(64)-4R (Siemens, Erlangen, Germany). Image registration was performed in 3D mode in a caudal direction with 2.5 minutes of registering per bed position. Reconstruction encompassed attenuation and scattering correction. The reconstruction method was as follows: True X + time-of-flight (TOF) and ultra-high-resolution positron emission tomography (PET) technology, two iterations, 21 subsets, Gaussian filter full width at half maximum 2.0 mm, image size 200 × 200 (matrix), zoom 1.0 and slice 3 mm. CT was performed before PET, without contrast enhancement, using the following parameters: voltage 120 kV, tube current 50, 150, or 200 mAs, pitch 0.8, and slice thickness 3 mm.

Measurement of standardised uptake value (SUV) is used widely to standardise oncological 2-[^{18}F]FDG PET/CT imaging. SUV_{max} values are calculated for region of interest (ROI) as the activity ratio (while considering its breakdown) per cubic centimetre. ROI was demarcated over an area of highest 2-[^{18}F]FDG uptake near the VGE (single measurement).

Target-to-background ratio (TBR) was defined as the ratio of SUV_{max} in the vicinity of the VGE and SUV_{max} of the blood pool region. The blood pool region was set in the centre of the ascending aorta, except when an inflammatory process enveloped the ascending aorta; in such cases, SUV_{max} was measured in the descending aorta.

Image interpretation

Two nuclear medicine physicians analysed all of the studies, and the results used in this work are the effect of consensus between them: in all cases, both physicians agreed.

Visual inspection of foci of increased uptake of 2-[18F]FDG PET/CT were recorded. Additionally, two visual grading scales were utilised: a five-grade scale formulated by Sah et al. [3] and a three-stage scale composed by Bowles et al. [4]. Both scales were based on an analysis of PET images, in which focal and intense uptake was associated with a high probability of infection, and low and diffuse uptake was associated with a low probability of infection. Inflammatory infiltration was defined as a metabolically active region with a density higher than fluid, and which is not naturally present in the area.

Statistical analysis

Statistical analysis was conducted using the permutation or Fisher test, depending on the type of variables tested. A p-value below 0.05 was considered the cut-off value for statistical significance. Due to the conducting of multiple hypothesis tests, p-value corrections were performed using a Benjamini–Hochberg algorithm with a false discovery rate (FDR) set to 0.05.

Statistical analysis was conducted on anonymised data in a Databricks environment using programming libraries including SparkR, ape, vegan, dplyr, hagis, purrr, arules, jmuOutlier, coin, perm, and data.table, ThresholdROC, and tibble.

Ethics

The authors declare no known competing financial interests or personal relationships that could influence the work reported in this article. This research received no specific grant from public or commercial sources. Work was conducted in agreement with the resolution of the Bioethical Commission at the Medical University of Lublin number KE-0254/228/2021 from 28.10.2021. No side effects were observed after the radionuclide procedure.

Results

Based on the authors' experience, three image patterns of VGEIs in the 2-[18F]FDG PET/CT study were defined, using the metabolic (PET) and morphological (CT) information. The images were analysed visually by assessing focality and metabolic activity, and semiquantitatively using the SUV_{max} values. 2-[18F]FDG uptake in the region of the VGE and metabolically active lymph nodes was evaluated. Moreover, typical infection signs in CT scans, such as gas bubbles, peri-graft fluid retention, thickening of the graft wall, adjacent blurred fat, soft tissue swelling, fistula, and pseudoaneurysms were observed.

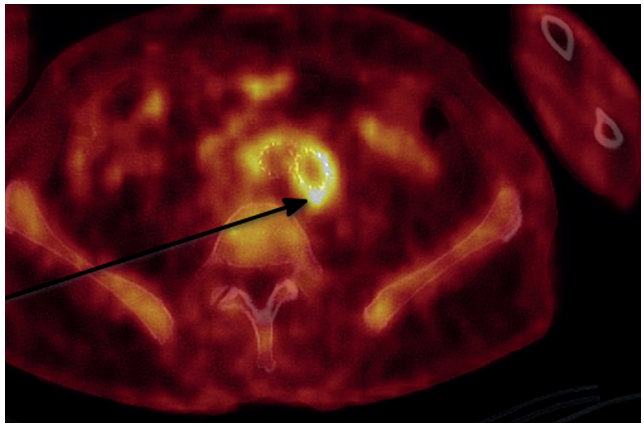

Figure 1. 2-[18F]FDG PET/CT fusion, transverse cross-section at the level of the iliac bones. Focal increase in metabolic activity in the posterior part of the aortobifemoral VE (marked by the arrow)

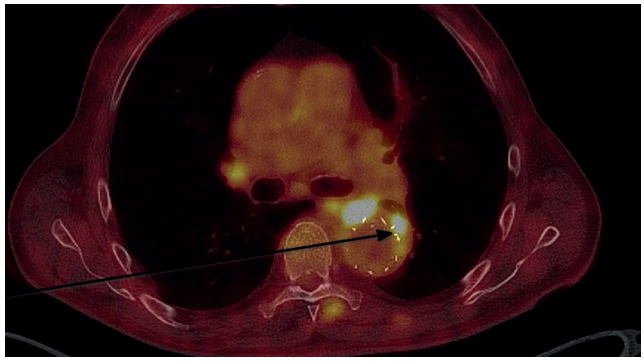

Figure 2. 2-[18F]FDG PET/CT fusion, transverse cross-section at the level of the mediastinum. Markedly increased metabolic activity in the VE wall, where both focal and diffuse uptake is observed (marked by the arrow)

First pattern (P1)

The first pattern (P1) was characterised by focally increased 2-[18F]FDG uptake in the area of the vascular graft (the activity should be at least twice the blood pool). This pattern is characterised by the absence of marked radiological signs of infection in CT scans (only a small amount of fluid and inflammatory infiltrate). An example of P1 is presented in Figure 1.

Second pattern (P2)

In this group of patients, diffusely increased uptake along the VGE with focally increased activity in PET images, as well as metabolically active lymph nodes, were observed. Additionally, in the CT images, the presence of fluid inflammatory infiltration can be observed. An example of P2 is presented in Figure 2.

Third pattern (P3)

As with P2, focally and diffusely increased activity in the VGE area was observed in P3. In CT, apart from extensive inflammatory

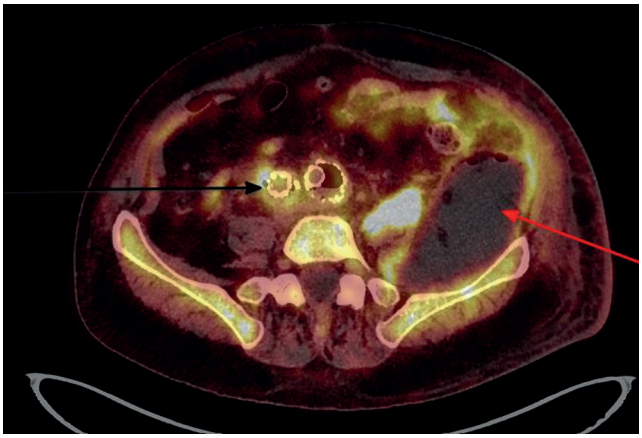

Figure 3. 2-[^{18}F]FDG PET/CT fusion, transverse cross-section at the level of the sacroiliac joints, markedly increased metabolic activity in the vicinity of the wall of the VE (black arrow) anteriorly to the left iliac bone large abscess (red arrow)

infiltrations and fluid collection, the presence of gas bubbles indicates purulent processes. An example of P3 is presented in Figure 3.

Additionally, an analysis of different 2-[^{18}F]FDG PET/CT image patterns (P1–P3) was performed. P1 was recognised in six patients; P2 and P3 were visible in 11 and 17 patients, respectively.

The SUV_{max} measurements were conducted in the area of the highest uptake of radiopharmaceuticals in the vicinity of the implanted VGE, which was established first by visual inspection and then by drawing the region within the same location and measuring SUV_{max}. The median SUV_{max} value in the vicinity of the implanted prostheses was 9.8 [IQR 6.1) for the study group. The values of median SUV_{max} were higher in the VE's than in VG's (SUV_{max} 10.2 (IQR 1.7) *vs.* SUV_{max} 9.0 (IQR 7.4) respectively], p = 0.003.

It was also observed that in the study group, the degree of uptake of 2-[^{18}F]FDG depends on location. A higher frequency of increased focal uptake of 2-[^{18}F]FDG was observed in the left arm of the aortobifemoral prosthesis than in the right (N = 9 *vs.* N = 4 — when the focus was in the arm of the prosthesis 70% were observed on the left and 30% on the right). However, the number of cases was too small to assess the statistical significance. Another common location of the increased 2-[^{18}F]FDG was part of the prosthesis located in the abdominal aorta (N = 12). The most common location of the increased 2-[^{18}F]FDG for the ascending aorta prosthesis was the aortic valve (the aortic valve was part of the prosthesis implanted during a Bentall procedure). The data is summarised in Table 2.

The median background SUV_{max} was 2.0 (IQR 0.7), while the TBR (the ratio of SUV_{max} in the area of infection and blood pool) was 4.6 (IQR 3.2) for the study group.

The most constant image signs of infection in the study group were focally increased (N = 33) and irregular uptake (N = 33) of a radiopharmaceutical. CT changes included inflammatory infiltration (N = 24) and gas bubbles (N = 19) in the VGE area. Infection could be recognised based on the visual grading scales described above. Additionally, there is a noticeable relation between the visual scale described above and those developed by Sah [3] and Bowles [4], where more advanced changes in one scale correspond to high levels in another. The data is summarised in Table 3.

The pattern types (P1–P3) described above were compared with laboratory data. The laboratory norm for C-reactive protein (CRP) was (0–5 mg/L) and for white blood cells (WBC) (4 000–10 000/L). Pattern level increased with the values of inflammatory markers indicating the severity of infection: in P1, median CRP was 60 (IQR 104.3) (mg/L) and WBC 13.3 (IQR 5.0) (/L); in P2, CRP 102.0 (IQR 106) (mg/L) and WBC 9.1 (IQR 106) (/L), and in P3, median CRP 110 (IQR 148.7) (mg/L) and WBC 14.5 (IQR 6.3) (/L). It was not possible

Table 2. Location of foci of increased 2-[^{18}F]FDG uptake in the vicinity of VGE in the study group

Part of aorta	Abdominal	Bifurcation	Left arm	Right arm	Aortic arch	Ascending
N	12	4	9	4	2	3

n — number of foci of increased 2-[^{18}F]FDG uptake

Table 3. SUV_{max} and TBR values depend on the level of visual grading scales

Visual grading scale by Sah	N	SUV_{max} in the area of infection		SUV_{max} of blood pool		TBR*		Level in author's scale	
		Median	IQR	Median	IQR	Median	IQR	Median	IQR
5	23	9.9	6.3	2.1	0.6	4.7	3	3	1
4	11	9	5.8	1.8	0.55	3.75	2.7	2	1
3	0								
2	0								
1	0								
Sum	34								
Visual grading scale by Bowles									
1	34	9.8	6.1	2	0.68	4.6	3.2	2.5	1
2	0								
3	0								
Sum	34								

*TBR — target-to-background ratio of SUV_{max} in the vicinity of suspected infection to the blood pool

Table 4. The authors' scale and its relation to the laboratory data

Authors' scale level	N pattern*	N CRP measurements**	N WBC measurements**	Median CRP (0–5) mg/L	IQR CRP mg/L	Median WBC (4 000–10 000) G/L	IQR WBC G/L
1	6	4	3	60.0	104.3	13.3	5.0
2	11	9	10	102.0	106.0	9.1	2.1
3	17	10	12	110.0	148.7	14.5	6.3

*N scale number of studies assigned to each pattern; ** number of CRP or WBC measurements acquired; CRP — C-reactive protein; WBC — white blood cells

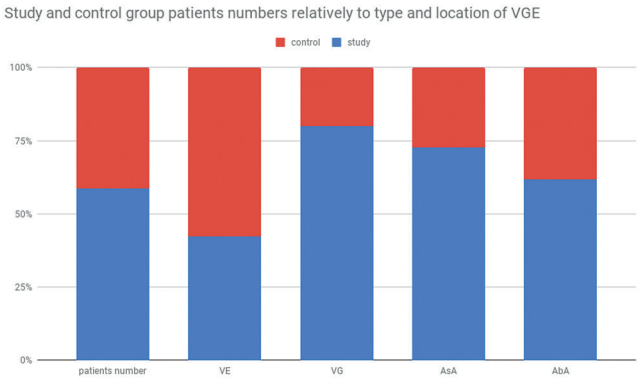

Figure 4. Study and control group patient numbers relative to type and location of vascular — graft; AbA — VGE that encompasses the abdominal aorta; AsA — VGE that encompasses the ascending Aorta; VE — vascular endograft; VG — vascular graft

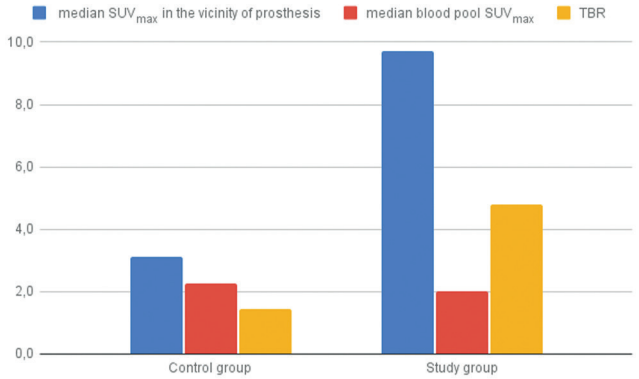

Figure 5. Comparison of SUV_{max} and TBR values in the study and control groups

to collect CRP and WBC measurements from all patients — 23 of 34 in the case of CRP and 25 of 34 for WBC. This, coupled with high variability in the data, meant that no statistical hypothesis testing was performed. The data is summarised in Table 4.

A statistically significant relationship was observed between infection frequency and type of VGE (the ratio of VE to VG in the control group was 19:5 and in the study group 7:10), with a p-value of 0.03. Although infections in the case of VE were less common, when they did occur, they usually did so with increased intensity as visualized on the image (median SUV_{max} in the area of infection for VG is 9 IQR 3.5 and 14,3 IQR 8 for VE). The data is summarised in Figure 4.

In the study group, SUV_{max} in the vicinity of suspected infection was 6.7 for silver-coated graft (one case), 10.1 (IQR 7.0) for synthetic, and 8.2 (IQR 2.6) for biological. The number of patients with each type of material prosthesis was insufficient to perform statistical tests.

We analysed the control group regarding metabolic activity in VGE's, SUV_{max} value, and TBR values, which were compared with the study group. Significantly higher values of activity were observed in the vicinity of the VGE median SUV_{max} in the study group was 9.8 (IQR 6.1) and TBR 5.3 (IQR 3.2), while in the control group, 3.1 (IQR 1.3) and 1.6 (IQR 0.5), respectively. The data is summarised in Figure 5 and Table 5.

Analysis of the image characteristics and SUV_{max} values revealed a statistically significant relationship between the presence of inflammatory infiltration in the study group and increased SUV_{max} values. The median SUV_{max} value in images with present inflammatory infiltration was 12.0 (IQR 5.5) and 9.0 (IQR 5.1) for images without infiltration ($p = 0.008$).

We also analysed the association rules to identify the most common occurrences of image characteristics. The most common pair of elements was the presence of gas bubbles with inflammatory infiltration. Other common pairs included inflammatory infiltration with metabolically active lymph nodes and inflammatory infiltration with fluid.

Discussion

The typical patient who requires implantation of a vascular prosthesis is a 65-year-old man [5]. Multiple factors influence the risk of infection, one of which is the location of the prosthesis. Increased prevalence of disease can be observed in cases of prostheses located in the inguinal area and distally to the inguinal ligament [6]. According to Bowles et al. [7], the frequency of infection for abdominal aorta prostheses is around 1%, and in the case of aortobifemoral 1.5–2%. Infections of vascular prostheses that encompass the thoracic aorta are relatively rare in the general population [8]. In the study group, patients with infection of the thoracic aorta constituted 23.5%, and in the control group, 12.5%. However, due to the relatively small sample size, the difference was not statistically significant.

Laboratory inflammatory markers like CRP and WBC in the case of VGEI are frequently in or slightly above the physiological range [9]. In this study, a wide range of values was observed. CRP ranged between 9 and 300 mg/L with a mean of 111.5 mg/L, while WBC in the study group ranged between 1600/L and 37 800/L with a mean of 13 600/L. In the authors' opinion, based on their experience, the severity of the VGEI measured by visual scales is not necessarily proportional to clinical or laboratory data.

According to the MAGIC guidelines, the diagnostic imaging study of choice is CT [10]. However, nuclear medicine studies are

Table 5. SUV_{max} and TBR values in the study and control groups

	N	SUV_{max}*			Blood pool SUV_{max}		TBR**		
		Median	IQR	p-value	Median	IQR	Median	IQR	p-value
Control group	24	3.1	1.3	0.003	2.3	0.5	1.6	0.5	0.003
Study group	34	9.8	6.1		2.0	0.7	5.3	3.2	

*SUV_{max} in the study group measured in the vicinity of the infection; in the control group, it was highest SUV_{max} in the vicinity of the prosthesis; **TBR — target-to-background ratio of SUV_{max} in the vicinity of suspected infection to the blood pool; in the control group, it was measured for maximal uptake in the vicinity of the prosthesis

emerging as a complementary option with higher specificity and sensitivity than pure CT scans [11]. CT achieves only 55% sensitivity for low-grade infections [12]. Moreover, in some patients, CT angiography (CTA) cannot be performed due to kidney or thyroid comorbidities; such contraindications are not present in the case of 2-[^{18}F]FDG PET/CT.

Interpretation of CT scans soon after implantation is complicated by the natural consequences of vascular graft procedure, such as the presence of fluid and gas bubbles [7]. Haematoma in the vicinity of a vascular prosthesis may be observed in 100% of patients after one week, but only 18% after 45 days and 10% 100 days after vascular procedure [13]. Further difficulties may be caused by metal artefacts [6].

Although CT scans are associated with a reduced per-study price relative to 2-[^{18}F]FDG PET/CT, performing nuclear medicine studies may lower costs by reducing the length and frequency of unnecessary hospitalisations [14].

2-[^{18}F]FDG PET/CT

Typically, uninfected vascular prostheses in 2-[^{18}F]FDG PET/CT are characterised by locally increased radiotracer accumulation due to the inflammatory component of the natural surgical wound healing process [14]. Definite differential diagnosis between crude and pathology-related increases in radiotracer uptake can be performed four to eight weeks after implantation [14]. In some cases, particularly when surgical adhesives are used [15], increased metabolism around vascular grafts may be present chronically [14]. The material of the vascular graft also influences 2-[^{18}F]FDG accumulation significantly. In the case of the vascular prostheses manufactured by Dacron, inhomogeneous uptake in the vicinity of the prostate may be physiological. The same image for the Gore-Tex device may indicate infection [16]. According to Keidar et al. [17], radiotracer uptake in prostheses manufactured from native veins diminishes over time; however, in the synthetic prosthesis, increased accumulation can last multiple years. In the current study, most patients had artificial, not silver-coated prostheses. This made it infeasible to establish the influence of VGE material.

Researchers have attempted to define a cut-off value of SUV_{max} that could help in the diagnosis of VGE infection. Depending on the study, those values have ranged from 3.8 to 8 [3, 18, 19]. In this study, the optimal value for the SUV_{max} that reduced the probability of false positive and false negative results was set to 6.8 and for TBR to 3.1. The thresholds calculated for VE were 8.0 (SUV_{max}), 3.6 (TBR) and for VG 6.0 (SUV_{max}), 3.2 (TBR).

The most critical image characteristic seen in cases of vascular graft infections is focally increased 2-[^{18}F]FDG uptake [3], which was present in 33 patients in the study group. Observing focally-increased uptake enables correct diagnosis in the early stages of infection. In the case of the MAGIC criteria, focal uptake in 2-[^{18}F]FDG PET/CT is a minor criterion and must be supported further by changes in the CT scan. According to those criteria, the most important image characteristic is the presence of gas bubbles (which, in the current study, was observed in 19 of the 34 patients). Although the presence of gas bubbles enables diagnosis with sensitivity (66–96%), the specificity ranges between 25 and 86% [19]. It is also worth mentioning that in the analysis of the association rules, gas bubbles frequently occurred with fluid and inflammatory infiltration. In the previous study the authors [2] found (what is further supported by the current one) that the presence of gas bubbles was linked to higher uptake of 2-[^{18}F]FDG ($p < 0.01$, SUV_{max} 11.8 ± 4.3 *vs.* 7.3 ± 2.8, 15 *vs.* 9 pts). Another conclusion of the previous study was that CT findings like gas bubbles, or peri-graft fluid retention were associated with significantly higher glucose metabolism; however, in some cases without anatomic alterations, increased metabolic activity was the only sign of infection.

The most significant contribution of this work is its establishment of a relationship between PET and CT changes in the three described patterns. Those patterns may serve as a new tool that enables patient risk stratification and diagnosis, thanks to the incorporation of both PET and CT data contrary to already established scales. Moreover, by incorporating holistic image analysis that includes patient data such as the type of material of the prosthesis and image characteristics described by both association rules and by the authors' patterns, as well as by semiquantitative analysis using SUV_{max} values, practitioners may be able to recognise vascular graft infection with increased confidence.

Conclusions

Comparative analysis of the study and control groups has revealed the utility of 2-[^{18}F]FDG PET/CT in diagnosing vascular prosthesis infections.

Developed patterns of VGEI have been summarised in a new three-level scale. In contrast to previous scales, this scale incorporates both CT and PET data which may enable reliable establishment of the severity of infection.

VEs were more common in the control group than in the study group. However, in the case of infection of the VE, signs of infection in 2-[^{18}F]FDG PET/CT were more severe.

Article information and declarations

Ethics statement

Work was conducted in agreement with the resolution of the Bioethical Commission at the Medical University of Lublin number KE-0254/228/2021 from 28.10.2021.

Funding

This research received no specific grant from public or commercial sources.

Conflict of interest

The authors declare no known competing financial interests or personal relationships that could influence the work reported in this article.

Supplementary material

None.

References

1. Israel O, Keidar Z. PET/CT imaging in infectious conditions. Ann N Y Acad Sci. 2011; 1228: 150–166, doi: 10.1111/j.1749-6632.2011.06026.x, indexed in Pubmed: 21718330.
2. Chrapko BE, Chrapko M, Nocuń A, et al. Patterns of vascular graft infection in 18F-FDG PET/CT. Nucl Med Rev Cent East Eur. 2020; 23(2): 63–70, doi: 10.5603/NMR.a2020.0015, indexed in Pubmed: 33007092.
3. Sah BR, Husmann L, Mayer D, et al. Diagnostic performance of 18F-FDG-PET/CT in vascular graft infections. Eur J Vasc Endovasc Surg. 2015; 49(4): 455–464, doi: 10.1016/j.ejvs.2014.12.024, indexed in Pubmed: 25648371.
4. Bowles H, Ambrosioni J, Mestres G, et al. Diagnostic yield of F-FDG PET/CT in suspected diagnosis of vascular graft infection: a prospective cohort study. J Nucl Cardiol. 2020; 27(1): 294–302, doi: 10.1007/s12350-018-1337-1, indexed in Pubmed: 29907934.
5. Fariñas MC, Campo A, Duran R, et al. Risk factors and outcomes for nosocomial infection after prosthetic vascular grafts. J Vasc Surg. 2017; 66(5): 1417–1426, doi: 10.1016/j.jvs.2017.06.078, indexed in Pubmed: 28823865.
6. Keidar Z, Nitecki S. FDG-PET in prosthetic graft infections. Semin Nucl Med. 2013; 43(5): 396–402, doi: 10.1053/j.semnuclmed.2013.04.004, indexed in Pubmed: 23905620.
7. Bowles H, Ambrosioni J, Mestres G, et al. Diagnostic yield of F-FDG PET/CT in suspected diagnosis of vascular graft infection: A prospective cohort study. J Nucl Cardiol. 2020; 27(1): 294–302, doi: 10.1007/s12350-018-1337-1, indexed in Pubmed: 29907934.
8. Sollini M, Berchiolli R, Delgado Bolton RC, et al. The "3M" approach to cardiovascular infections: multimodality, multitracers, and multidisciplinary. Semin Nucl Med. 2018; 48(3): 199–224, doi: 10.1053/j.semnuclmed.2017.12.003, indexed in Pubmed: 29626939.
9. Wassélius J, Malmstedt J, Kalin Bo, et al. High 18F-FDG uptake in synthetic aortic vascular grafts on PET/CT in symptomatic and asymptomatic patients. J Nucl Med. 2008; 49(10): 1601–1605, doi: 10.2967/jnumed.108.053462, indexed in Pubmed: 18794261.
10. Lyons O, Baguneid M, Barwick TD, et al. Diagnosis of aortic graft infection: a case definition by the management of aortic graft infection collaboration (MAGIC). Eur J Vasc Endovasc Surg. 2016; 52(6): 758–763, doi: 10.1016/j.ejvs.2016.09.007, indexed in Pubmed: 27771318.
11. Folmer EIR, Meijenfeldt GV, Laan MJV, et al. Diagnostic imaging in vascular graft infection: a systematic review and meta-analysis. Eur J Vasc Endovasc Surg. 2018; 56(5): 719–729, doi: 10.1016/j.ejvs.2018.07.010, indexed in Pubmed: 30122333.
12. Spacek M, Belohlavek O, Votrubova J. Diagnostics of "non-acute" vascular prosthesis infection using 18F-FDG PET/CT: our experience with 96 prostheses. Eur J Nucl Med Mol Imaging. 2009; 36(5): 850–858, doi: 10.1007/s00259-008-1002-z, indexed in Pubmed: 19107480.
13. Legout L, D'Elia PV, Sarraz-Bournet B, et al. Diagnosis and management of prosthetic vascular graft infections. Med Mal Infect. 2012; 42(3): 102–109, doi: 10.1016/j.medmal.2012.01.003, indexed in Pubmed: 22341664.
14. Guenther SPW, Cyran CC, Rominger A, et al. The relevance of 18F-fluorodeoxyglucose positron emission tomography/computed tomography imaging in diagnosing prosthetic graft infections post cardiac and proximal thoracic aortic surgery. Interact Cardiovasc Thorac Surg. 2015; 21(4): 450–458, doi: 10.1093/icvts/ivv178, indexed in Pubmed: 26174118.
15. Schouten LRA, Verberne HJ, Bouma BJ, et al. Surgical glue for repair of the aortic root as a possible explanation for increased F-18 FDG uptake. J Nucl Cardiol. 2008; 15(1): 146–147, doi: 10.1016/j.nuclcard.2007.11.009, indexed in Pubmed: 18242493.
16. Keidar Z, Engel A, Hoffman A, et al. Prosthetic vascular graft infection: the role of 18F-FDG PET/CT. J Nucl Med. 2007; 48(8): 1230–1236, doi: 10.2967/jnumed.107.040253, indexed in Pubmed: 17631553.
17. Keidar Z, Pirmisashvili N, Leiderman M, et al. 18F-FDG uptake in noninfected prosthetic vascular grafts: incidence, patterns, and changes over time. J Nucl Med. 2014; 55(3): 392–395, doi: 10.2967/jnumed.113.128173, indexed in Pubmed: 24516259.
18. Tokuda Y, Oshima H, Araki Y, et al. Detection of thoracic aortic prosthetic graft infection with 18F-fluorodeoxyglucose positron emission tomography/computed tomography. Eur J Cardiothorac Surg. 2013; 43(6): 1183–1187, doi: 10.1093/ejcts/ezs693, indexed in Pubmed: 23333838.
19. Zogala D, Rucka D, Ptacnik V, et al. How to recognize stent graft infection after endovascular aortic repair: the utility of 18F-FDG PET/CT in an infrequent but serious clinical setting. Ann Nucl Med. 2019; 33(8): 594–605, doi: 10.1007/s12149-019-01370-9, indexed in Pubmed: 31144118.